Transmitter-in-the-Loop Optimization of Physical Radar Emissions

John Jakabosky[1], Shannon D. Blunt[1], Matthew R. Cook[1,2], James Stiles[1], and Sarah A. Seguin[1]

[1]Radar Systems Lab, University of Kansas, Lawrence, KS
[2]Garmin International, Olathe, KS

Abstract – **Ongoing work is exploring the optimization of physical radar emissions based on the continuous phase modulation (CPM) implementation of polyphase codes. Here a modification to the code search strategy known as Marginal Fisher's Information (MFI) is presented that enables this greedy approach to further improve upon the performance of the resulting CPM-implemented continuous waveform in terms of range sidelobes. The optimization process is also expanded to include the effects of the transmitter (from both modeled and physical hardware perspectives) to facilitate the optimization of physical emissions that are specifically tuned to the transmitter. This approach is particularly useful for high-power transmitters in which the actual physical emission is a spectrally modified and non-linearly distorted version of the intended radar waveform.**

I. INTRODUCTION

It was recently shown [1] that the continuous phase modulation (CPM) implementation of polyphase radar codes [2] provides a means with which to optimize the resulting non-linear FM (NLFM) waveform via determination of the code values. While the method of optimization is arbitrary, in [1] the Marginal Fisher's Information (MFI) algorithm [3] was employed as its greedy structure enables rapid convergence to a solution of sufficient quality. It should be noted that the solution obtained by MFI is generally a local optimum as the nature of the code search problem would necessitate searching over all possible solutions to ensure global optimality. That said, if a locally optimal solution meets the design specifications, then it is clearly sufficient.

In [1] the optimized NLFM waveforms were shown to achieve a range ambiguity performance of better than a -30 dB peak sidelobe level (PSL) for a waveform generated from a polyphase code of 65 chips. Here, two modifications to the greedy MFI search strategy are presented that enable the determination of waveforms with PSL better than -40 dB for the same underlying code length. Note that this result is obtained <u>without</u> the use of any form of amplitude weighting and thus no SNR loss is incurred.

Radar waveforms do not provide the complete picture of what the radar physically emits. Radar transmitters, particularly those operating at high power, are known to induce some distortion upon the waveform that can result in increased range sidelobes [5] and spectral leakage [6]. This distortion is caused by the spectral shaping and non-linear

effects of the components in the transmitter. For example, legacy radars rely heavily on vacuum tube technology to serve as power amplifiers due to the prohibitive costs of upgrades as well as the power limitations on solid state amplifiers. The high efficiency of these tubes comes at the cost of distortion to the waveform.

To address the deleterious effects that a high power transmitter may impose, one may either a) incorporate some form of waveform predistortion, or b) incorporate the operation of the transmitter into the optimization of the radar emission. This paper focuses upon the latter. Note that, just as the concepts of discrete 'codes' and continuous 'waveforms' were delineated in [1], so too here is the intended waveform and the resulting physical emission treated separately due to the influence of transmitter distortion.

The general framework for emission optimization is depicted in Figure 1. A polyphase code is selected and subsequently implemented (here using CPM) to generate a continuous waveform. This waveform is injected into the transmitter to generate the physical emission that is launched from the radar antenna. It is this physical emission for which performance is assessed to drive the optimization process. Note that for this paper we only consider a loopback configuration that does not include the antenna and platform effects. These specific effects are particularly important for scenarios in which mutual coupling impacts the temporal emission (e.g. MIMO [7]).
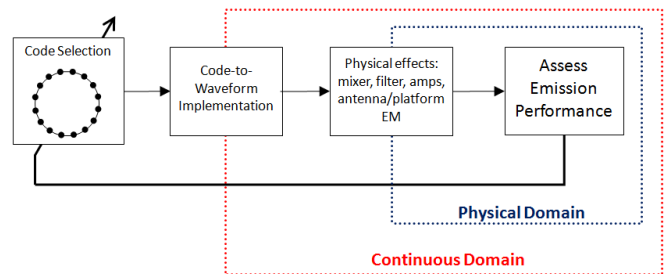

Figure 1. Transmitter-in-the-loop emission optimization

Incorporation of the transmitter into the optimization process may be achieved in two possible ways: *model-in-the-loop* and *hardware-in-the-loop*. The model-in-the-loop approach is more efficient as there is no need for the data handling overhead of generating the physical waveform on the hardware and subsequently capturing the resulting emission

after the transmitter in each optimization iteration. That said, there is a limit on the fidelity with which a model can represent the physical system. In contrast, while the hardware-in-the-loop approach may be less efficient to execute, it encompasses all of the eccentricities of the individual transmit hardware. The best overall approach is most likely one that first employs model-in-the-loop to efficiently reach a near-optimal solution followed by hardware-in-the-loop optimization for fine tuning.

The paper is organized as follows. Section II provides a brief description of the CPM implementation of polyphase codes while Section III presents the waveform optimization approach and recent results afforded by modifications to the search strategy. In Section IV the model-in-the-loop and hardware-in-the-loop approaches are discussed followed by corresponding results for each in Section V.

II. CPM RADAR IMPLEMENTATION

Continuous phase modulation (CPM), originally conceived for use in power and spectrally efficient communications, has been modified to enable the implementation of polyphase radar codes as continuous waveforms [1,2]. The general structure of the CPM implementation for radar is shown in Figure 2 where the input $p(t)$ is a train of N impulses with separation T_p such that the total pulse width is $T = NT_p$.

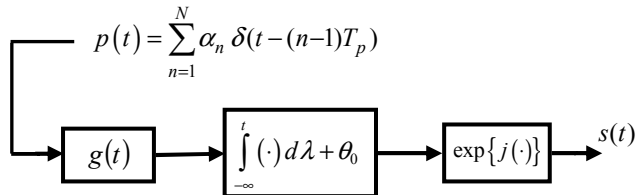$$p(t) = \sum_{n=1}^{N} \alpha_n \, \delta(t - (n-1)T_p)$$

Figure 2. CPM implementation for radar

The shaping filter $g(t)$ can be any arbitrary shape as long as it has temporal support on $[0, T_p]$ and is scaled to integrate to unity (rectangular and raised cosine are the most common for communications [8]). The nth impulse is weighted by symbol α_n, which is the amount of phase change between successive chips as determined by

$$\alpha_n = \begin{cases} \tilde{\alpha}_n & \text{if } |\tilde{\alpha}_n| \leq \pi \\ \tilde{\alpha}_n - 2\pi \, \text{sgn}(\tilde{\alpha}_n) & \text{if } |\tilde{\alpha}_n| > \pi \end{cases}, \quad (1)$$

where

$$\tilde{\alpha}_n = \theta_n - \theta_{n-1} \quad \text{for} \quad n = 1, \cdots, N, \quad (2)$$

sgn($\cdot$) is the signum operation, and θ_n is the phase of the nth element in a length $N+1$ polyphase code. The first code element θ_0 is included as the initial condition for the integration stage. Hence, where θ_n for $n = 0, 1, \ldots, N$ are the $N+1$ phase values in the code, the values α_n for $n = 1, 2, \ldots, N$ are the N phase transitions. The output $s(t)$ is the baseband non-linear FM (NLFM) waveform that is modulated onto the carrier. The performance of this waveform is thus optimized by determining the proper sequence of θ_n (or α_n) values with

which to drive the CPM implementation. Note that the scheme in Figure 2 is from [1] which differs slightly from the original CPM radar implementation given in [2].

III. WAVEFORM OPTIMIZATION

Conceptually, the marginal Fisher's information (MFI) approach is to separately modify each individual parameter, with all others held constant, such that its marginal contribution to the overall 'error' is minimized. Assuming the use of a matched filter on receive, the error here arises from the range sidelobes. From an implementation standpoint, MFI is a greedy search that, while not guaranteed to achieve global optimality, has still been observed to obtain very good locally optimal solutions for problems where the search space is prohibitively large [3, 9].

For the polyphase code search problem, MFI examines each individual chip to determine the best phase value from a discrete constellation while all other chips are held constant. This process is then repeated for a different chip until there are no single changes that could further improve the code. Here, the "goodness" of each chip value is assessed by measuring the autocorrelation sidelobes of the continuous waveform $s(t)$ that is produced by the CPM implementation of the candidate code as in Figure 2 (the inclusion of transmitter effects as depicted in Figure 1 are addressed in the next section). The CPM implementation stage (and corresponding assessment) adds additional computational cost to the search process, a driving factor in the use of this efficient optimization approach.

Here we consider modifications to the MFI search to further increase search speed and the quality of the solution by 1) performing the per-chip optimization in the order of greatest improvement (i.e. dynamic ordering of chip selection) and 2) employing a line search algorithm to reduce the number of constellation phase values to assess. In fact, it is the efficiency gained by the latter that makes the former feasible.

To search the constellation of phases for a given chip, we consider the use of a Fibonacci line search [10], which is known to provide the fastest search of a unimodal function. Of course, the assessment of waveform autocorrelation sidelobes as a function of an underlying code phase value is not necessarily unimodal. A practical solution to this limitation is to divide the 2π phase search space into sections, perform a line search on each of these smaller sections, and then compare the set of results. Here the phase search space is divided into 4 equal sections. Thus, the constellation value providing the maximum marginal improvement can be found more rapidly than by searching the entire constellation, particularly when the constellation is large. For example, full enumeration would require that a 1024-value constellation have double the search time of one with 512. In contrast, the Fibonacci search requires only one additional evaluation.

The speed improvement afforded by the Fibonacci search for the phase value of a single chip makes it computationally feasible to dynamically determine the order in which the chips are selected. Thus, at a given point within the optimization

process, the particular chip selected is the one that, by modifying its phase value, can provide the greatest marginal improvement in the range sidelobes. Of course, to make this determination requires that the search process be independently performed on all chips so that the best can be selected. This strategy effectively squares the number of per-chip searches, hence the need for the Fibonacci search.

To demonstrate the capability of this search strategy consider the optimization of the CPM implementation of an N = 64 length polyphase code with a 256-point constellation. The process is initialized with a P4 code [4, pp. 126-128], the CPM implementation of which is known to produce a standard LFM waveform. The optimization was performed as in [1] by alternating the design metric (i.e. the measure of error) between peak sidelobe level (PSL) and integrated sidelobe level (ISL) after each round of modifying the complete set of chips until no further improvement was possible. The range ambiguity for the initial LFM waveform and for the resulting optimized NLFM (O-NLFM) waveform is compared in Figure 3 (with a close-up view of the mainlobe and nearest sidelobes in Figure 4).
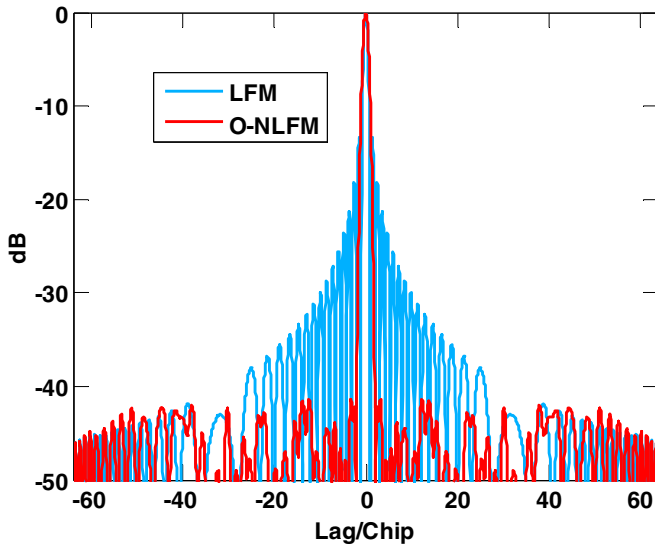

Figure 4. Range ambiguity for LFM and optimized NLFM (detail view)

Figure 3. Range ambiguity for LFM and optimized NLFM
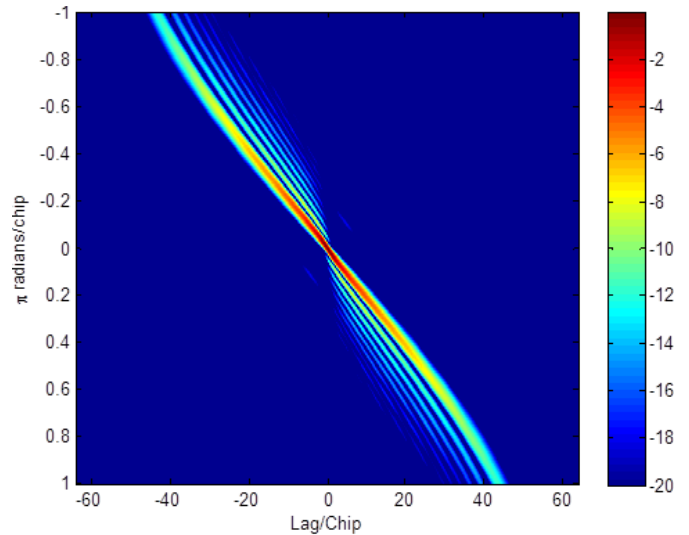
Figure 5. Range-Doppler ambiguity for optimized NLFM (highest 20 dB)

As one would expect [4, pp. 86-96], the optimized NLFM (O-NLFM) waveform yields a resolution degradation relative to LFM. Specifically, using the 3dB width of the mainlobe as reference, O-NLFM is 30% wider than LFM. However, compared to the -13.5 dB PSL of LFM, this trade-off has enabled a nearly 28 dB improvement such that the O-NLFM waveform yields a PSL of -41.4 dB. With regard to integrated sidelobe level (ISL), the LFM performance of -9.8 dB is markedly exceeded by the -26.1 dB of the O-NLFM waveform. These improvements were made while maintaining a Time-Bandwidth Product of approximately N+1 = 65. Finally, Figure 5 illustrates the range-Doppler ambiguity (the highest 20 dB) of O-NLFM which shows that Doppler tolerance is largely preserved.
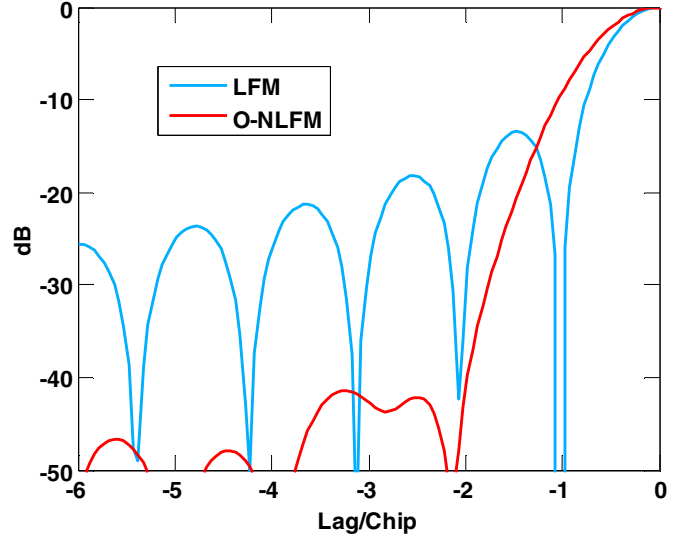
IV.   TRANSMITTER-IN-THE-LOOP OPTIMIZATION

The radar transmitter is comprised of multiple components (mixers, filters, amplifiers, etc.) that can, to varying degrees, distort the intended waveform. The most prominent source of distortion tends to be the power amplifier, which produces non-linear amplitude compression as a result of being operated well into saturation to meet requirements for high power emissions (particularly for long range sensing).

There are essentially two ways in which the transmitter may be incorporated into the process of optimizing the radar emission: 1) a model-in-the-loop formulation in which a mathematical model of the transmitter is used and 2) direct use of hardware-in-the-loop. The former has the benefit of a simpler implementation that subsequently leads to higher optimization efficiency (i.e. realization of waveforms based on longer codes with denser constellations). However, the

model-in-the-loop approach cannot account for all the characteristics of the transmitter and thus there is a limit to the fidelity that it can provide. Conversely, the hardware-in-the-loop approach allows for the emission to be precisely tuned to the physical hardware, though the physical generation of candidate waveforms and the subsequent capture of their emission from the transmitter introduce additional complexity into the optimization process. Both approaches are considered in the following.

A. Model-in-the-Loop Optimization

The simplest approach for transmitter model-in-the-loop optimization can be realized using an IIR filter such as a Chebyshev filter followed by a mathematical model of the amplitude compression provided by the power amplifier. The filter serves to bandlimit the waveform much like it would be by a physical system as well as providing a more realistic rise and fall time for the pulse and the amplitude ripple and phase distortion of a physical system. The power amplifier causes further distortion that compounds the effects of filtering the waveform.

Extensive work exists on modeling power amplifier distortion. Here we shall use the model of a solid stage amplifier from [11] as it approximates the physical amplifier to be used for the hardware-in-the-loop approach. Note that greater distortion can be expected for tube-based power amplifiers.

Denoting $s_{in}(t)$ as the filtered version of the waveform that is input to the power amplifier, the model-based emission can be expressed as

$$s_{out}(t) = s_{in}(t) \, G[s_{in}(t)] \,, \tag{3}$$

where the compression term $G[\bullet]$ is defined as

$$G[r] \triangleq \frac{A(|r|)}{|r|} \tag{4}$$

and

$$A(r) = \frac{vr}{\left[1 + \left(\dfrac{vr}{A_0}\right)^{2p}\right]^{1/2p}} \,. \tag{5}$$

In (5), v is the small-signal gain, A_0 is the saturating amplitude at the amplifier output, and p is an integer that controls the softness of transition from linear to non-linear.

B. Hardware-in-the-Loop Optimization

Direct incorporation of the physical transmitter into the optimization process is considered a superior solution as it naturally accounts for all of the eccentricities that one may not be able to capture with a mathematical model. For this work, one channel of the four channel radar testbed depicted in Figure 6 is used (a photo of this setup is shown in Figure 7).
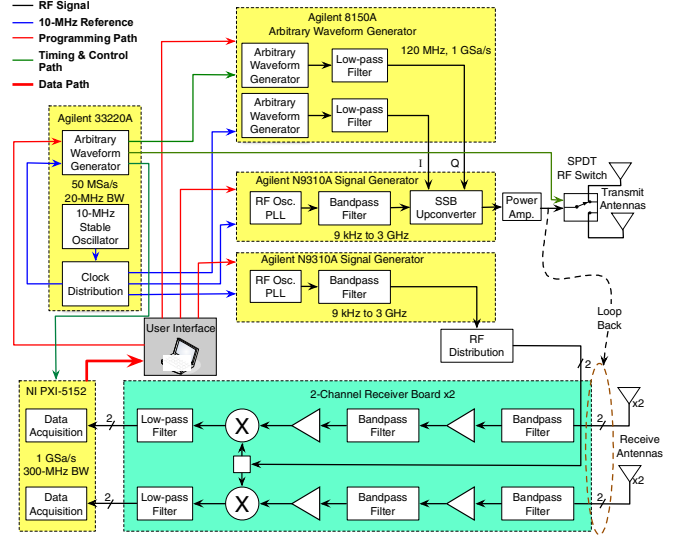

Figure 6. System diagram of radar testbed

Figure 7. Photo of radar testbed

To mimic relatively high power within a loopback configuration, a power amplifier and loopback channel is used as depicted in Figure 6. Following the CPM implementation of a candidate code (performed digitally in Matlab), the resulting waveform is first converted to in-phase and quadrature-phase (I/Q) components and then loaded onto the arbitrary waveform generator (AWG). The AWG drives the waveform into a single sideband (SSB) modulator that up-converts the waveform to S-band. The up-converted waveform is then passed through the solid-state power amplifier (operated in saturation) and then an attenuator before being "received" and down-converted. The subsequent baseband signal is sampled by the digitizer and passed back to Matlab (running on the laptop in Figure 7) where the range ambiguity of this candidate emission is assessed. It is assumed that any distortion induced within the receive chain is negligible in comparison to that introduced by the transmitter.

V. EMISSION OPTIMIZATION RESULTS

To assess the efficacy of the transmitter-in-the-loop optimization schemes, an "idealized" waveform was first designed under the assumption of an ideal distortionless transmitter and the initialization of an LFM waveform (P4 code implemented with CPM). Note that the optimization of these idealized waveforms and the subsequent versions to be optimized with the transmitter-in-the-loop schemes rely upon the previous MFI approach described in [1] (i.e. without the modifications described in Section III which are recent to the writing of this paper). For both optimization schemes, the range sidelobe level of the idealized waveform is assessed along with that of the idealized waveform after being passed through the respective transmitter (model or hardware). Using the idealized waveform as an initialization, the optimization process is then repeated for each transmitter-in-the-loop scheme to obtain a tuned emission for each.

A. Assessment of Model-in-the-Loop Optimization

For the model-in-the-loop scenario, the CPM-implemented waveform generated by a length $N = 64$ code with a 256-point constellation is optimized. For an LFM initialization ('seed waveform') and under the assumption of an ideal transmitter, the range sidelobes described by the blue curves in Figures 8 and 9 are realized. The PSL of this idealized waveform is found to be -35.8 dB. If this same waveform is injected into the model from Section IV (with parameters v=30, A_0=1 and p=3), the resulting emission yields the red range sidelobes in Figures 8 and 9 and a PSL that has degraded by 2.6 dB to -33.2 dB.

When the optimization process is repeated, using the idealized waveform as initialization and including the model within the optimization loop, the PSL loss is almost completely eradicated. This model-in-the-loop emission realizes the black range sidelobes in Figures 8 and 9 that provide a PSL of -35.4 dB, only 0.4 dB from the idealized case.
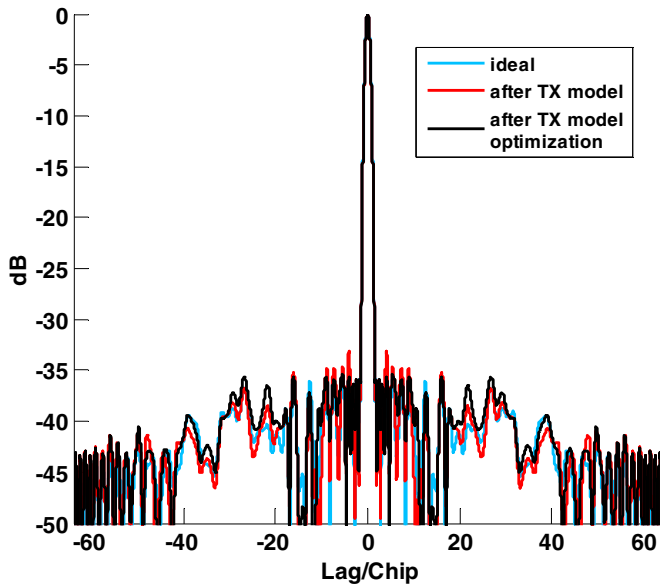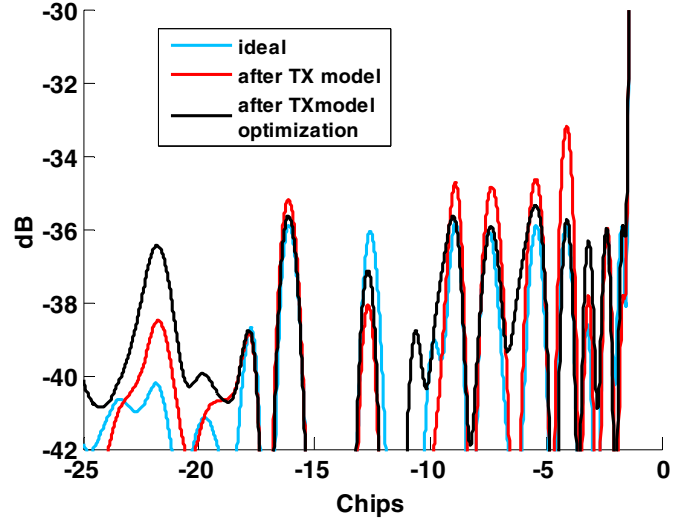

Figure 9. Range ambiguity for model-in-the-loop optimization (detail)

B. Assessment of Hardware-in-the-Loop Optimization

For the hardware-in-the-loop scenario, the CPM-implemented waveform generated by a length $N = 20$ code with a 32-point constellation is optimized. The shorter code length and constellation density used here relative to the model-in-the-loop scenario is due to the longer optimization time caused by the additional overhead of including hardware. Again using an LFM initialization and under the assumption of an ideal transmitter, the blue range sidelobes shown in Figures 10 and 11 are obtained having a PSL of -28.6 dB. When this idealized waveform is injected into the physical transmitter, the resulting emission produces the red range sidelobes in Figures 10 and 11 that realize a 4.7 dB degradation to a PSL of -23.9 dB.

Using the idealized waveform as initialization, repeating the optimization process with the physical hardware included in the loop produces an emission with the black range sidelobes in Figures 10 and 11. The hardware-in-the-loop emission yields a PSL of -28.0 dB, thus recovering 4.1 dB of lost sensitivity due to distortion

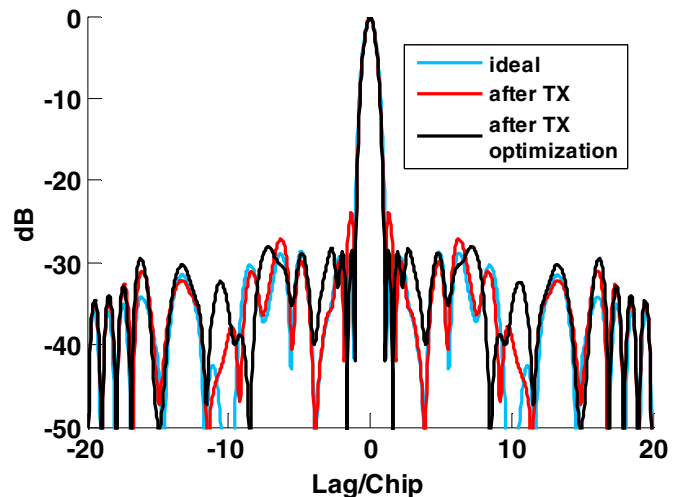Figure 8. Range ambiguity for model-in-the-loop optimization

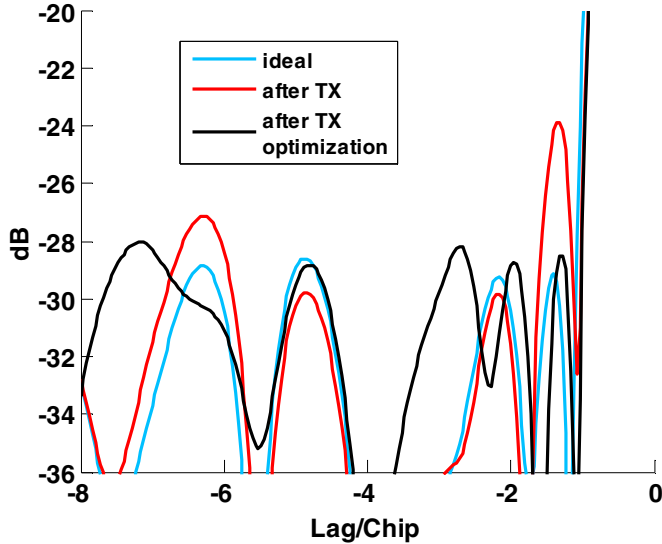Figure 10. Range ambiguity for hardware-in-the-loop optimization

Figure 11. Range ambiguity for hardware-in-the-loop optimization (detail)

VI. CONCLUSIONS

It has been shown that the optimization of polyphase-coded continuous waveforms implemented via the continuous phase modulation (CPM) structure provides a means to obtain waveforms with excellent range ambiguity performance while maintaining constant amplitude. Waveforms with better than -41 dB PSL were achieved with a Time-Bandwidth Product of 65. Furthermore, this overall framework readily allows for inclusion of the transmitter into the optimization process via either model-in-the-loop or hardware-in-the-loop paradigms. Ongoing work is exploring the impact of waveform spectral shaping, tube-based transmitters, and more exotic emission schemes such as MIMO.

REFERENCES

[1] J. Jakabosky, P. Anglin, M.R. Cook, S.D. Blunt, and J. Stiles, "Non-linear FM waveform design using marginal Fisher's information within the CPM framework," *IEEE Radar Conference*, Kansas City, MO, 23-27 May 2011.

[2] S. Blunt, M. Cook, E. Perrins, and J. de Graaf, "CPM-based radar waveforms for efficiently bandlimiting a transmitted spectrum" *IEEE Radar Conference,* Pasadena, CA, 4-8 May 2009.

[3] J. D. Jenshak and J. M. Stiles, "A fast method for designing optimal transmit codes for radar," *IEEE Radar Conference*, Rome, Italy, 26-30 May 2008.

[4] Levanon and E. Mozeson, *Radar Signals*, IEEE Press, 2004.

[5] C.E. Cook and J. Paolillo, "A pulse compression predistortion function for efficient sidelobe reduction in a high-power radar," *Proc. IEEE*, vol. 52, no. 4, pp. 377-389, Apr. 1964.

[6] H. Griffiths, L. Cohen, S. Watts, E. Mokole, C. Baker, M. Wicks, and S. Blunt, "Radar spectrum management and engineering issues: regulatory and technical approaches," in preparation for *Proc. IEEE*.

[7] B. Cordill, J. Metcalf, S.A. Seguin, D. Chatterjee, and S.D. Blunt, "The impact of mutual coupling on MIMO radar emissions," *IEEE Intl. Conf. Electromagnetics in Advanced Applications*, Turino, Italy, 12-17 Sept. 2011.

[8] J.B. Anderson, T. Aulin, and C.-E. Sundberg, *Digital Phase Modulation*, Plenum Press, 1986.

[9] J. Stiles and J. Jenshak, "Sparse array construction using marginal Fisher's information," *Intl. Waveform Diversity & Design Conf.*, Orlando, FL, 8-13 Feb. 2009.

[10] D. E. Ferguson, "Fibonaccian searching", *Communications of the ACM,* vol. 3, no. 12, pp. 648, Dec. 1960.

[11] E. Costa, M. Midrio, S. Pupolin, "Impact of amplifier nonlinearities on OFDM transmission system performance," *IEEE Communications Letters*, vol. 3, no. 2, pp. 37-39, Feb. 1999.